Immunity
Article

S100A8-S100A9 Protein Complex Mediates Psoriasis by Regulating the Expression of Complement Factor C3

Helia B. Schonthaler,[1] Juan Guinea-Viniegra,[1] Stefanie K. Wculek,[1] Isabel Ruppen,[2] Pilar Ximénez-Embún,[2] Ana Guío-Carrión,[1] Raquel Navarro,[3] Nancy Hogg,[4] Keith Ashman,[2,5] and Erwin F. Wagner[1,*]
[1]BBVA Foundation–CNIO Cancer Cell Biology Programme, Spanish National Cancer Research Centre (CNIO), 29029 Madrid, Spain
[2]Proteomics Unit, Spanish National Cancer Research Centre (CNIO), 29029 Madrid, Spain
[3]Department of Dermatology, Hospital Universitario La Princesa, 28006 Madrid, Spain
[4]Leukocyte Adhesion Laboratory, London Research Institute, Cancer Research UK, London WC2A 3LY, UK
[5]Present address: University of Queensland Centre for Clinical Research, Building 71/918, Royal Brisbane & Women's Hospital Campus, Herston, 4029-QLD, Australia
*Correspondence: ewagner@cnio.es
http://dx.doi.org/10.1016/j.immuni.2013.11.011

SUMMARY

Psoriasis is a common heterogeneous inflammatory skin disease with a complex pathophysiology and limited treatment options. Here we performed proteomic analyses of human psoriatic epidermis and found S100A8-S100A9, also called calprotectin, as the most upregulated proteins, followed by the complement component C3. Both S100A8-S100A9 and C3 are specifically expressed in lesional psoriatic skin. S100A9 is shown here to function as a chromatin component modulating C3 expression in mouse and human cells by binding to a region upstream of the *C3* start site. When S100A9 was genetically deleted in mouse models of skin inflammation, the psoriasis-like skin disease and inflammation were strongly attenuated, with a mild immune infiltrate and decreased amounts of C3. In addition, inhibition of C3 in the mouse model strongly reduced the inflammatory skin disease. Thus, S100A8-S100A9 can regulate C3 at the nuclear level and present potential new therapeutic targets for psoriasis.

INTRODUCTION

Psoriasis is a chronic recurrent disabling skin disease that affects approximately 2% of the population. The prototypic form of psoriasis is characterized by persistent plaques of inflamed and scaly skin. The initial trigger(s) leading to the development of psoriasis are currently unknown. However, it has been demonstrated that both the innate and adaptive immune systems play roles in the pathophysiology of psoriasis (Di Meglio et al., 2011; Lowes et al., 2007). Several mouse models of psoriasis, targeting either immune cells or keratinocytes have been developed, constituting powerful tools to dissect the underlying molecular mechanisms that trigger aspects of this disease (Arwert et al., 2012; Wagner et al., 2010). A better understanding of tumor necrosis factor-α (TNF-α) activation in psoriasis, mediated by the tissue inhibitor of metalloproteinase 3 (TIMP)-3 and TNF-α converting enzyme (TACE) pathway, came from the analyses of the inducible AP-1-dependent psoriasis-like mouse model (Guinea-Viniegra et al., 2009; Zenz et al., 2005). Constitutive epidermal deletion of *Junb* and *Jun* in this model led to massively increased TNF-α shedding, mediated by reduced amounts of TIMP-3, which rendered high activity of TACE. TIMP-3 was shown to be a direct transcriptional target of JunB and Jun (Guinea-Viniegra et al., 2009). In psoriasis, AP-1 activity is impaired in lesional skin (Johansen et al., 2004) and JunB expression is heterogeneous within lesional epidermis (Zenz et al., 2008).

The calcium-binding proteins S100A7 (Psoriasin), S100A8 (MRP-8), and S100A9 (MRP-14) are located in the psoriasis susceptibility locus 4 (PSORS4) and are highly expressed at sites of acute and chronic inflammation (Nacken et al., 2003), including psoriasis (Guttman-Yassky et al., 2008; Swamy et al., 2010). A mouse model with switchable overexpression of S100A7 and S100A15 displayed psoriasis-like symptoms upon stress (Wolf et al., 2010), indicating that S100A proteins are potential mediators of psoriasis. Targeted disruption of S100A8 in mice caused lethality early in development (Baker et al., 2011). In contrast, mice lacking S100A9 are viable, fertile, and are overall healthy with a mild peripheral neutropenia (Hobbs et al., 2003; Manitz et al., 2003).

S100A9 together with S100A8 forms a heterodimeric complex (Leukert et al., 2006), termed calprotectin, whose molecular functions are not well understood. The extracellular function of S100A8-S100A9 is well documented as being a potent chemoattractant in mice and antimicrobial in humans (Nakatsuji and Gallo, 2011). S100A8 and S100A9 bind to several receptors including RAGE and CD36 (Gebhardt et al., 2008; van Lent et al., 2009), thereby affecting downstream signaling through NF-κB and AP-1 (Gebhardt et al., 2006; Grivennikov et al., 2010). These proteins were also identified as downstream targets of NF-κB in carcinogenesis (Németh et al., 2009). The S100A8-S100A9 complex is expressed in epithelial tissues, as well as in monocytes and granulocytes (Hobbs et al., 2003). In the skin, basal amounts of calprotectin are very low, whereas it is highly expressed during wound healing and in inflammatory conditions like in psoriasis (Kerkhoff et al., 2012).

Based on an unbiased proteomic analysis of psoriatic epidermis, here we showed a functional link between S100A8-S100A9

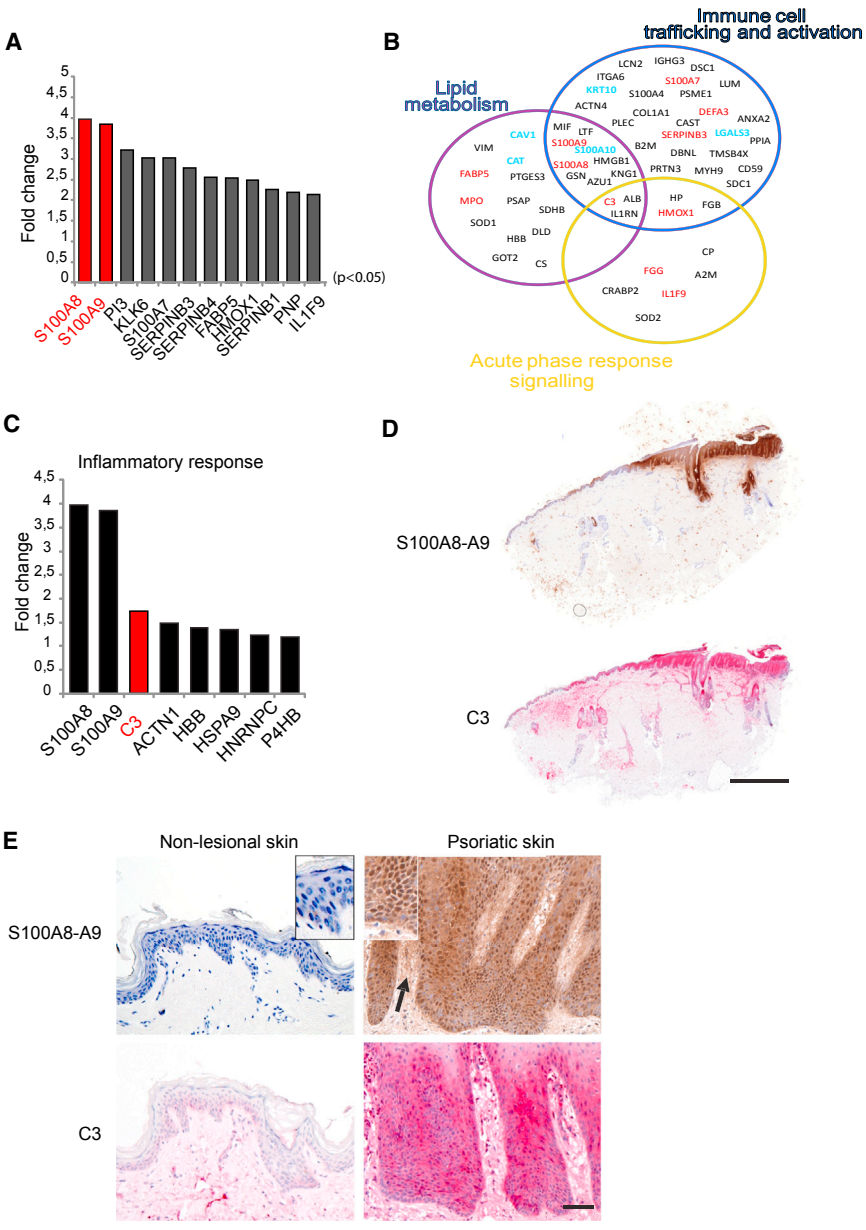

Figure 1. The Epidermal Proteome in Psoriasis

(A) Top 12 upregulated proteins identified by iTRAQ in psoriasis ($p < 0.05$ considered significant).

(B) Depicted are differentially regulated proteins identified in human psoriatic epidermis linked to lipid metabolism, immune cell trafficking, and activation and acute phase response signaling (red, upregulated; blue, downregulated; black proteins have been identified, but no significant regulation).

(C) Upregulated inflammatory proteins identified in the human epidermal proteome ($p < 0.05$).

(D) Immunohistochemical (IHC) stainings for S100A8-S100A9 and C3 on biopsies of psoriatic patients covering nonlesional, perilesional, and lesional skin (n = 6). Scale bar represents 2,000 μm.

(E) IHC for human S100A8-S100A9 in nonlesional and lesional skin from psoriatic patients. Scale bar represents 50 μm. (E; arrow indicates extracellular S100A8-S100A9 staining; n = 10). See also Figure S1.

and the alternative complement pathway composed of the complement component C3 and the complement factor B (CFB). By using primary mouse and human keratinocytes and mouse models for skin inflammation and psoriasis, we showed that S100A8-S100A9 modulated C3 expression by binding to the promoter. Loss of S100A8-S100A9 and/or blocking C3 led to prevention of the psoriasis-like phenotype, which provides potential therapeutic targets for psoriatic patients.

RESULTS

The Epidermal Proteome in Psoriasis

Psoriasis has a highly complex pathophysiology and it has been demonstrated that a disturbed interaction between immune cells and keratinocytes underlies the disease symptoms (Nestle et al., 2009). To identify new therapeutic targets in the psoriatic epidermis, we analyzed epidermal samples of lesional and nonlesional skin of 19 psoriasis vulgaris patients (psoriasis area severity index > 15) by using an unbiased iTRAQ (isobaric tag for relative and absolute quantitation) approach. By using this methodology, 1,217 proteins could be identified (see Figure S1A available online) and 214 of these proteins were significantly differentially regulated in lesional compared to nonlesional epidermis. S100A8 and S100A9 were the most upregulated epidermal proteins in lesional epidermis (Figure 1A). This upregulation of S100A9 was confirmed by protein immunoblotting (data not shown). Bioinformatic analyses revealed that more than 11% of the identified differentially regulated proteins are linked to interleukin-1β (IL-1β) function (25/214 proteins) (Figure S1B). Moreover, the 214 proteins were sorted according to their canonical functions and pathways with IPA (Ingenuity Pathways Analysis). This clustering revealed that three major biological functions, previously implicated in psoriasis, were altered: immune cell trafficking and activation, acute phase response, and lipid metabolism (Figure 1B). The complement factor C3 was identified as being functionally involved in all three of these biological processes (Acevedo and Hammar, 1989; Basset-Séguin et al., 1993; Wyatt et al., 1989). Besides S100A8-S100A9, the complement factor C3 was within the most significantly upregulated inflammatory proteins in psoriatic epidermis (Figure 1C). Importantly, RNA analyses of C3 and the C3-activation partner complement factor B (CFB) and of IL-1β in psoriatic patient samples revealed consistently increased concentrations (Figures S1C–S1E). Immunohistochemical (IHC)

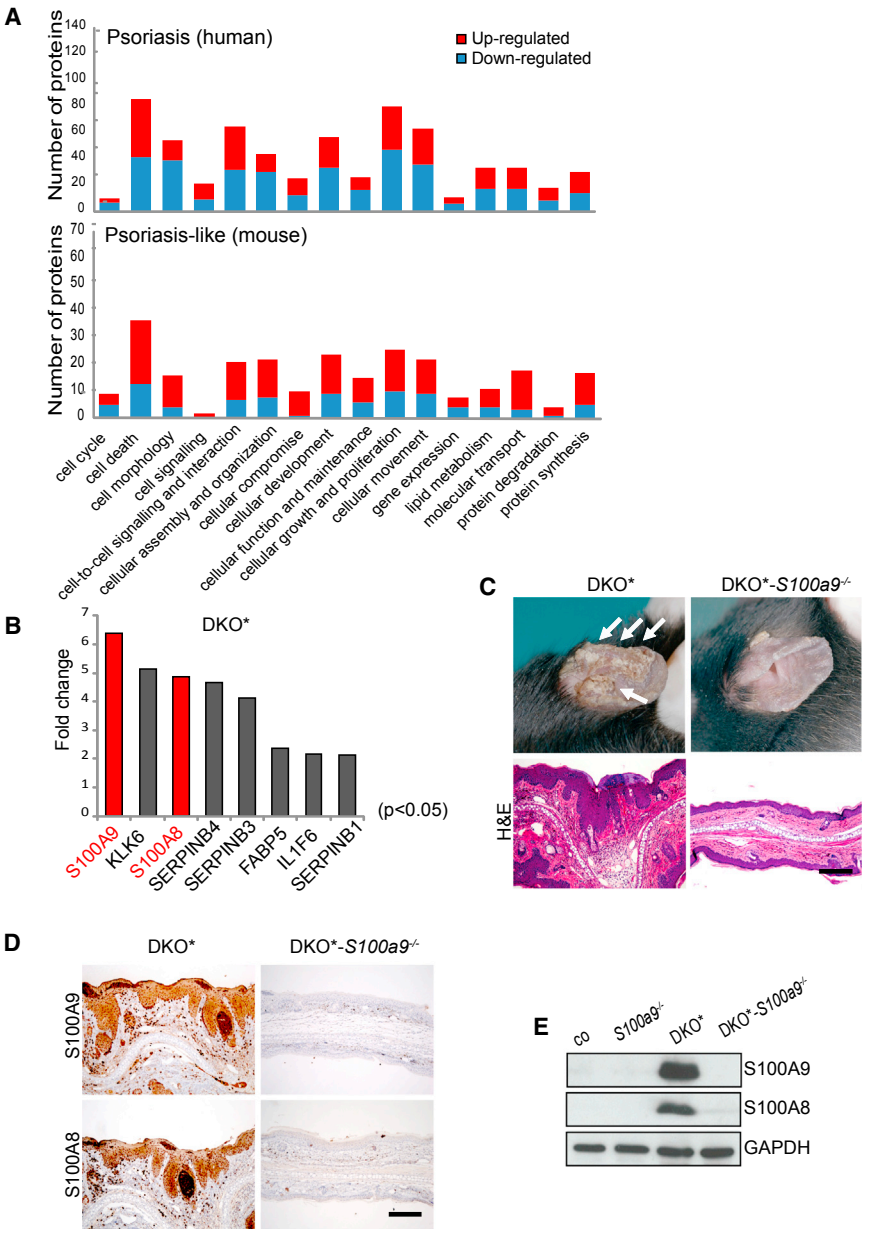

Figure 2. Role of S100A9 in Psoriasis-like Disease

(A) Differentially regulated proteins sorted according to their cellular function in psoriatic and DKO* samples. Bars represent the different cellular function; the number of upregulated proteins is shown in red, and the number of downregulated proteins within this cellular function is shown in blue.

(B) Top-upregulated proteins in DKO* mice according to the top-upregulated proteins identified by iTRAQ in psoriatic epidermal samples ($p < 0.05$).

(C) Macroscopic phenotype of DKO* mice (n = 20) and DKO*-*S100a9*$^{-/-}$ mice (n = 20); arrows indicate scaly plaques on the ear surface. H&E staining of ear sections 18 days after the last tamoxifen injection.

(D) S100A9 and S100A8 shown by IHC on mouse ear sections (scale bars represent 50 μm).

(E) Protein immunoblotting of S100A8 and S100A9 from total ear (n = 10 each). See also Figure S2.

staining for S100A8-S100A9 with an antibody recognizing the S100 dimer on biopsies from psoriatic patients covering nonlesional, perilesional, and lesional skin showed a specific increase in perilesional to lesional areas (Figures 1D and 1E). Moreover, IHC staining for C3 on the same biopsies revealed a similar expression pattern compared to S100A8-S100A9 (Figures 1D and 1E), suggesting that both proteins are likely involved in psoriasis pathophysiology and progression. Double labeling of S100A8-S100A9 and CD45 and C3 and CD45 identified keratinocytes, and to lesser extent immune cells, as the major source of S100A8-S100A9 and C3 protein (Figure S1F).

To determine whether the induction of S100A8-S100A9 is able to activate C3 and CFB expression in a cell-autonomous manner, we knocked down *JUNB* and *JUN* in primary neonatal human keratinocytes similar to the previously described mouse cells (Zenz et al., 2005). *JUNB* and *JUN* knockdown induced high expression of S100A8-S100A9 leading to strong upregulation of C3 and a significant increase in CFB and of IL-1β (Figure S1G). These results suggest a potential causal link between S100A8-S100A9-mediated induction and expression of C3 in the development of psoriasis.

Differentially regulated proteins identified in the iTRAQ approach clustered in psoriasis susceptibility regions (PSORS), when sorted according to their location in the human genome (Figure S2A). Furthermore, *JUN* (PSORS7), *JUNB* (PSORS2), *S100A8-S100A9* (PSORS4), and C3 (PSORS2) are all located in PSORS, emphasizing a potential causal link of these proteins in psoriasis (Figure S2A).

To mechanistically define a possible molecular link between S100A8-S100A9 and C3, we first employed the previously described inducible psoriasis-like mouse model (DKO* for inducible, epidermal double deletion of *Junb* and *Jun*). All mutant mice were maintained on a mixed genetic background for more than 15 generations, and only littermates were used as controls. In this mouse model, S100A8 and S100A9 proteins were upregulated prior to the onset of the disease symptoms and IL-1β concentrations were also induced in the diseased epidermis (Guinea-Viniegra et al., 2009; Schonthaler et al., 2009; Zenz et al., 2005). iTRAQ analysis of epidermis from DKO* mice was performed as for the human samples. The comparison of the differentially regulated proteins ($p < 0.05$) from psoriasis and the psoriasis-like disease, which were clustered according to their regulation obtained in the iTRAQ analysis and their cellular functions, revealed a highly similar pattern (Figure 2A). This indicates that the impairments in cellular functions observed in psoriatic epidermis are manifested

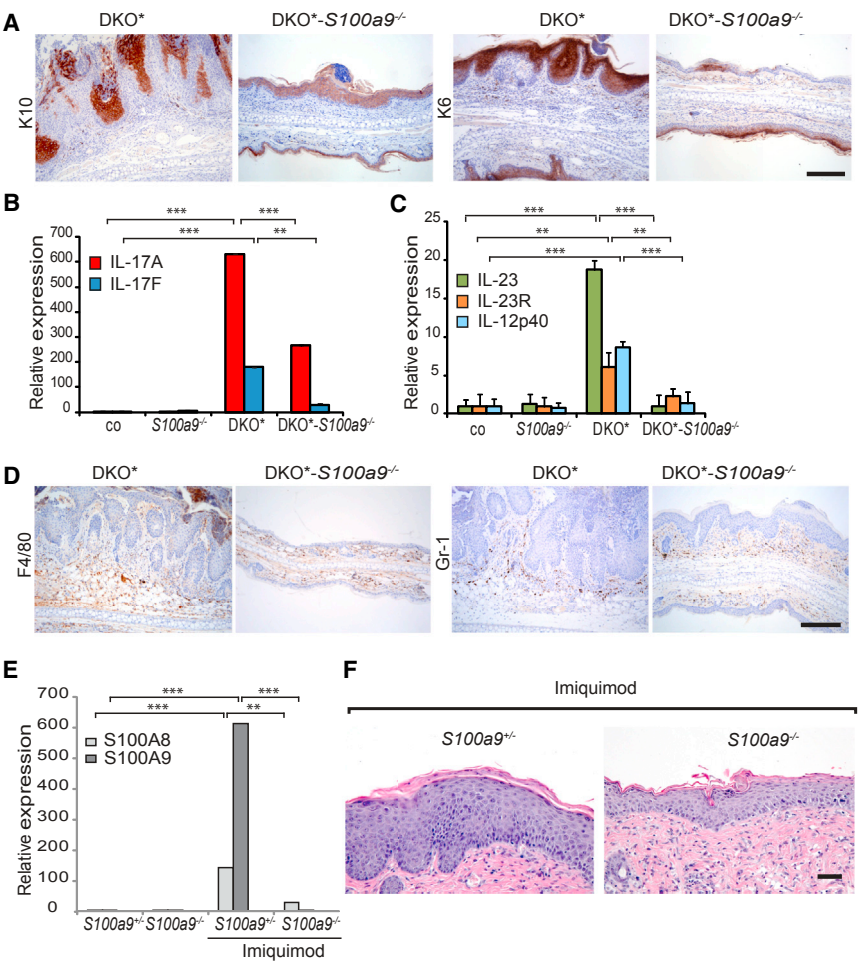

Figure 3. Phenotypic Characterization and Role of S100A9 after Imiquimod Treatment

(A) IHC on ear sections for keratin 10 and keratin 6 in DKO* and DKO*-*S100a9*$^{-/-}$mice. Scale bar represents 50 μm.

(B) IL-17A and IL-17F levels and (C) IL-23, IL-23R, and IL-12p40 levels (n = 4–6 each) in co, DKO*, *S100a9*$^{-/-}$, DKO*, and DKO*-*S100a9*$^{-/-}$mice. Error bars represent SD.

(D) IHC for myeloid markers F4/80 and Gr-1. Scale bar represents 50 μm.

(E) RT-PCR analyses for S100A8-S100A9 RNA in control and s100a9/ mice after Imiquimod treatment.

(F) H&E staining of back skin from Imiquimod-treated control and S*100a9*$^{-/-}$ mice (scale bar represents 50 μm). RT-PCR analyses for S100A8-S100A9 RNA in control and S*100a9*$^{-/-}$ mice after Imiquimod treatment. Error bars represent SD. Statistical analyses are described in Experimental Procedures. See also Figure S3.

in the psoriasis-like mouse model. Furthermore, this analysis identified S100A8-S100A9 within the top three upregulated proteins in mouse epidermis displaying a psoriasis-like phenotype (Figure 2B).

Role of S100A8-S100A9 in Psoriasis

To functionally analyze the role of S100A8-S100A9 in psoriasis pathogenesis, we genetically deleted *S100a9* in the DKO* psoriasis-like mouse model (DKO*-*S100Aa9*$^{-/-}$) (Figure S2B). In the absence of S100a9, a significant improvement of the psoriasis-like symptoms was observed (Figure 2C; Figures S2C and S2D). Macroscopically, scaly plaques on the ears and tails of triple-knockout mice DKO*-*S100a9*$^{-/-}$ were absent (arrows in Figure 2C). The skin architecture of ears and tails of DKO*-*S100a9*$^{-/-}$ mice was almost unaffected with minor hyper- and parakeratosis, (Figure 2C; data not shown). We have previously shown that S100A8-S100A9 were rapidly upregulated 3 days after the last Tam injection in DKO* mice and prior to the onset of the symptoms (Zenz et al., 2005). When monitoring DKO*-*S100a9*$^{-/-}$ mice for approximately 1 month after the last injection, no changes in the phenotype were observed.

Protein immunoblotting and immunohistochemical (IHC) analyses for epidermal S100A8 and S100A9 showed a strong induction in DKO* mice (Figures 2D and 2E; data not shown). S100A8 was not detectable by protein immunoblotting, IHC, and selective reaction monitoring (SRM) mass spectrometry (MS) analysis in DKO*-*S100a9*$^{-/-}$ mice, which is in agreement with previous results (Hobbs et al., 2003) (Figures 2D and 2E; data not shown).

Proliferation assessed by Ki67 staining was significantly decreased in the basal layer of the epidermis of DKO*-*S100a9*$^{-/-}$ compared to DKO* mice, but not completely reverted to control levels (data not shown). Analyses of epidermal markers for differentiation (keratin 10) and stress response (keratin 6) by IHC (Figure 3A) and RT-PCR (data not shown) showed that proper epidermal differentiation had recovered and that the stress response was reduced thereby reflecting the macroscopically improved phenotype. Importantly, absence of *S100a9* in DKO* mice markedly decreased amounts of IL-17A, IL-17F, IL-23, IL-23R, and IL-12p40 (Figures 3B and 3C); *Il1b* RNA and serum concentrations were also reduced (Figures S2E and S2F). Congruently, DKO*-*S100a9*$^{-/-}$ mice displayed a significant reduction of multiple immune cell types in the skin compared to DKO* mice. This was evident from IHC staining for F4/80^{+}, Gr-1^{+}, CD4^{+}, and CD8^{+} cells and was also reflected in the significantly reduced numbers of myeloid peroxidase (MPO)$^{+}$ cells in both epidermal and dermal samples (Figure 3D; Figures S3A and S3B). Intraepidermal T cells, a hallmark of psoriasis observed in skin biopsies, were also seen in DKO* skin and found reduced in skin sections from DKO*-*S100a9*$^{-/-}$ mice (data not shown). This indicates that the immune response, an essential initiator of psoriasis, is diminished due to the loss of S100A8-S100A9.

In addition, the Imiquimod-induced skin inflammation model (Palamara et al., 2004; Suzuki et al., 2000; van der Fits et al., 2009) was used to validate the function of S100A9 in a second mouse model. Although this model has limitations reflecting the hallmarks of psoriasis, it does show a strong upregulation

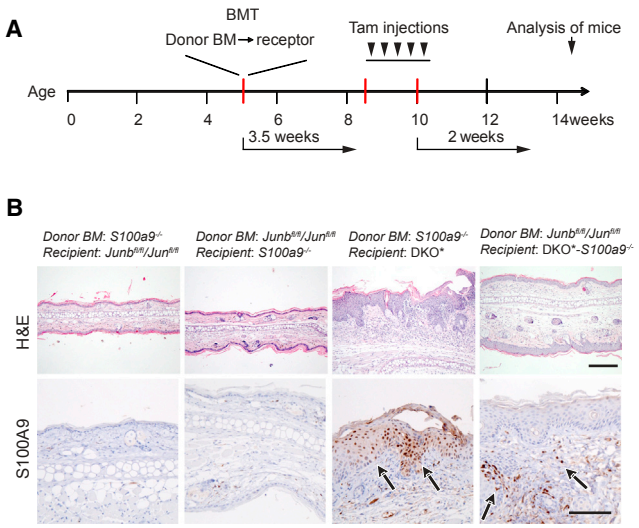

Figure 4. Contribution of Immune Cells to Psoriasis-like Phenotype

(A) Scheme of experimental procedure for bone marrow transplantation experiments.

(B) H-E staining on ear sections of the different transplantation groups (n = 3). IHC staining for S100A9 in the different transplantation groups (n = 3; BM: bone marrow; scale bars represent 50 μm). See also Figure S4.

of S100A8-S100A9 (Figure 3E). Loss of S100A9 resulted in reduced epidermal thickening (Figure 3F; data not shown), demonstrating that S100A8-S100A9 play an important role in promoting the local inflammatory processes leading to a psoriasis-like inflammatory phenotype.

Serum analyses of cytokines produced by keratinocytes and implicated in immune cell recruitment in psoriasis, namely IL-22, M-CSF, GM-CSF, CCL20 (Tohyama et al., 2009), VEGF, CCL2, and RANTES, were significantly increased in DKO* mice (Wagner et al., 2010) (Schonthaler et al., 2009) and data not shown). A subset of these cytokines—CCL2, RANTES, and TNFα—was reduced in DKO*-*S100a9*$^{-/-}$ mice (Figure S3C). These results demonstrate the role of S100A8-S100A9 and their downstream signaling in the amplification of the immune response to develop the psoriasis-like skin disease.

The importance of both, epidermal, as well as immune cell-derived, S100A8-S100A9 in triggering the psoriasis-like disease was analyzed by transplanting *S100a9*$^{-/-}$ bone marrow into DKO* mice and vice versa (Figure 4; Figure S4). Bone marrow transplantations were performed 3.5 weeks prior to the induction of the phenotype to secure engraftment (Figure 4A). *S100a9*$^{-/-}$ bone marrow (BM) was transplanted into *Junb*$^{fl/fl}$ and *Jun*$^{fl/fl}$ mice, as well as *Junb*$^{fl/fl}$ and *Jun*$^{fl/fl}$ BM into *S100a9*$^{-/-}$ mice to control for side effects of the transplantation procedure. No side effects were observed, and the mice did not develop any changes when compared to control mice (Figure 4B). Importantly, chimeric DKO* mice with transplanted *S100a9*$^{-/-}$ BM displayed reduced psoriasis-like symptoms (Figure 4; Figure 2C). The phenotype was not abolished, and chimeric DKO*-*S100a9*$^{-/-}$ mice carrying *Junb*$^{fl/fl}$ and *Jun*$^{fl/fl}$ BM did not show strongly increased psoriasis-like symptoms (Figures 4A and 4B; Figures S4A–S4C). Thus, S100A8-S100A9 produced by both keratinocytes and immune cells is required to develop the psoriasis-like disease.

Complement Component C3 Is Induced by S100A8-S100A9

To investigate how S100A8-S100A9 regulate the local immune response resulting in a psoriasis-like skin disease, we next performed an unbiased iTRAQ quantitative proteomic analysis on isolated epidermis of controls, *S100a9*$^{-/-}$, DKO*, and DKO*-*S100a9*$^{-/-}$ mice. This analysis identified 94 proteins ($p < 0.05$) that were elevated in the DKO* mice and reverted to control levels in DKO*-*S100a9*$^{-/-}$ mice. These 94 proteins were sorted according to their canonical functions and pathways with IPA. This clustering revealed that immune cell trafficking and activation, acute phase response, and lipid metabolism (Figure 5A) were affected as seen in the iTRAQ analysis of psoriatic epidermis. The complement factor C3 was found to be significantly downregulated in DKO*-*S100a9*$^{-/-}$ mice in this proteomic screening (Figures 5A and 5B). Although the prolyl 4-hydroxylase beta protein (P4HB) was also significantly affected in DKO*-*S100a9*$^{-/-}$ mice, it could not be linked to the three biological functions (Figure 5B). These data suggest that C3 is an essential effector downstream of S100A8-S100A9 in inflammation.

Consistent with the proteomic analysis, C3 mRNA upregulation was observed in isolated DKO* epidermis, but not in DKO* *S100a9*$^{-/-}$ mice (Figure 5C). To identify which complement activation pathway was modulated by loss of S100A8-S100A9, we analyzed RNA of different components of the complement activation pathways. Complement factor C1r, for example, remained upregulated in DKO*-*S100a9*$^{-/-}$ epidermis (Figure 5D). However, complement factor B (CFB), an activator of C3 in the alternative complement pathway, was regulated similarly to C3 (Figure 5D). CFB associates with C3 to form the C3 convertase, cleaving C3 molecules into C3a and C3b subunits, thereby activating and enhancing the pathway (Markiewski and Lambris, 2007). Protein immunoblot analysis of epidermal extracts of DKO* mice revealed a change in the band pattern of C3, indicating its cleavage and activation (Figure S5A). A significant increase in C3b specific peptides in DKO* epidermis compared to controls was also detected in the proteomic analysis, providing further evidence for C3 activation (Figure S5B). Thus, S100A8-S100A9 is an effective regulator of C3 in skin inflammation.

The S100A8-S100A9, C3, Axis in Keratinocytes In Vitro

To analyze whether S100A8-S100A9 and C3 function cell autonomously in keratinocytes, we induced upregulation of S100A8-S100A9 in primary mouse keratinocytes by deleting *Junb* and *Jun* by using adenoviruses expressing Cre recombinase (Ad-Cre) (DKO) (Figure 5E; Figure S5C). High amounts of S100A8-S100A9 in DKO keratinocytes were accompanied by increased C3 and CFB levels (Figures 5F and 5G; Figures S5D and S5E), whereas C1r levels remained unaltered (Figure S5F). IL-1β concentrations were elevated along with enhanced Caspase-1 activity (Figures S5G and S5I). Increased amounts of IL-1β protein were also detected by ELISA in DKO cell culture supernatants (Figure S5H). Importantly, DKO-*S100a9*$^{-/-}$ keratinocytes showed significantly reduced amounts of RANTES and CCL2 (Figure S5J), two known downstream effectors of C3 (Markiewski and Lambris, 2007; Monsinjon et al., 2003; Venkatesha et al., 2005). Moreover, primary keratinocytes treated

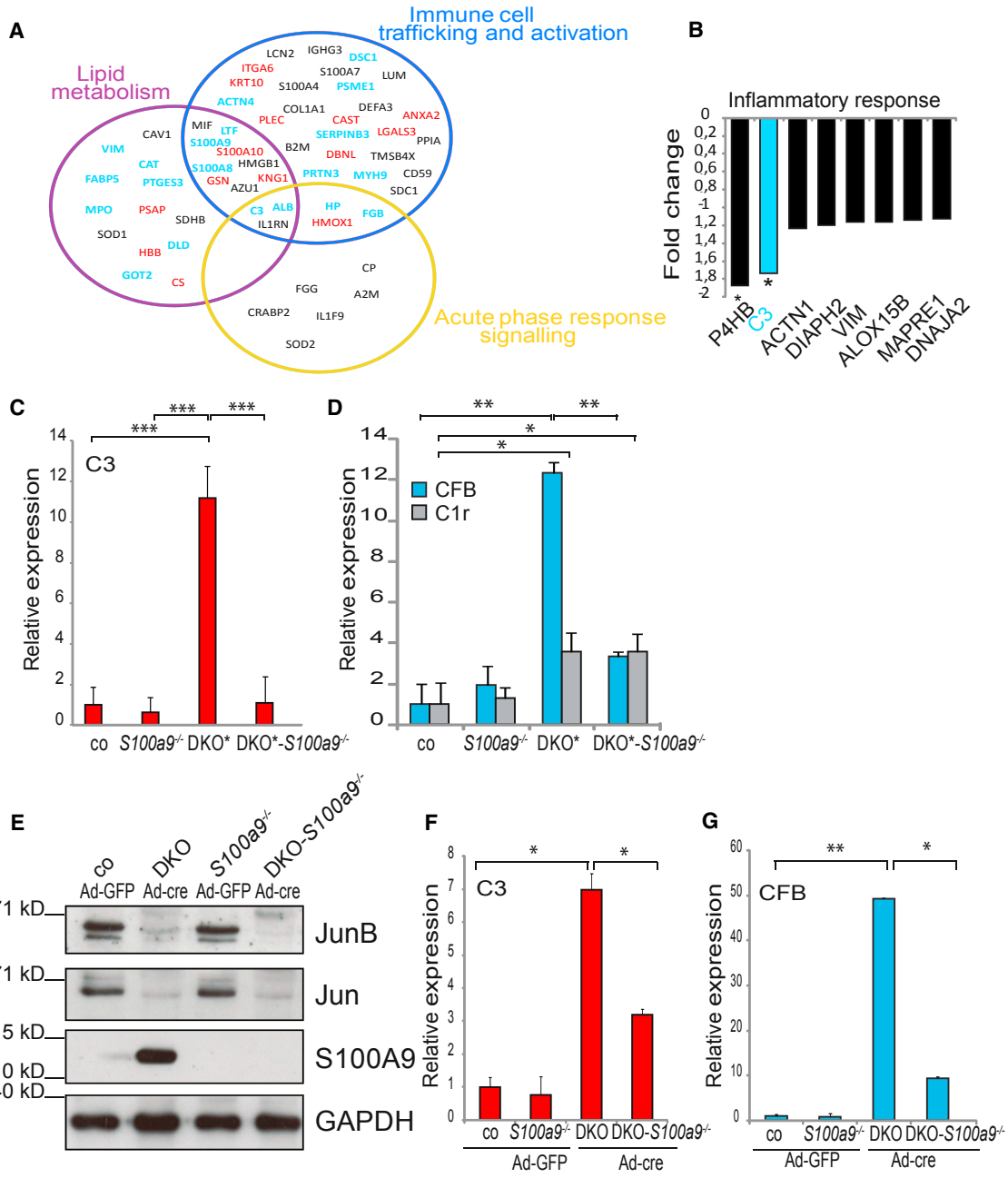

Figure 5. Identification of Downstream Effectors of S100A8-S100A9

(A) iTRAQ analysis: differentially regulated proteins in DKO*-S100a9$^{-/-}$ mice compared to DKO*, linked to immune cell trafficking and activation, acute phase response signaling, and lipid metabolism (upregulated proteins in red, downregulated proteins in blue; proteins in black were identified, but not significantly regulated).

(B) Significantly downregulated inflammatory response proteins in DKO*-*S100a9*$^{-/-}$ compared to DKO* (*$p < 0.05$) identified by iTRAQ. RT-PCR analysis of C3 (C) (n = 4–6 each), CFB, C1r (n = 4–6 each).

(D) RNA amounts in ear and tail epidermis of controls, *S100a9*$^{-/-}$, DKO*, and DKO*-*S100a9*$^{-/-}$ mice. Error bars represent SD.

(E) Protein immunoblotting for Jun and JunB in primary mouse keratinocytes after Adeno-cre (Ad-cre) treatment (n = 5).

(F and G) RT-PCR analysis of C3 (F) and CFB (G) after Adeno-cre-mediated (Ad-cre) knockout of *Jun* and *Junb* (DKO) in cultured mouse keratinocytes in controls, *S100a9*$^{-/-}$, DKO*, and DKO*-*S100a9*$^{-/-}$ (n = 4). Error bars represent SD. See also Figure S5.

with lipopolysaccharide (LPS) or flagellin displayed induced S100A8-S100A9 expression (Abtin et al., 2010; Javkhlan et al., 2011) and increased amounts of C3 and IL-1β (data not shown). These data indicate that expression of S100A8-S100A9 and C3-CFB is regulated in a cell-autonomous manner in keratinocytes, strongly suggesting an important role in psoriasis.

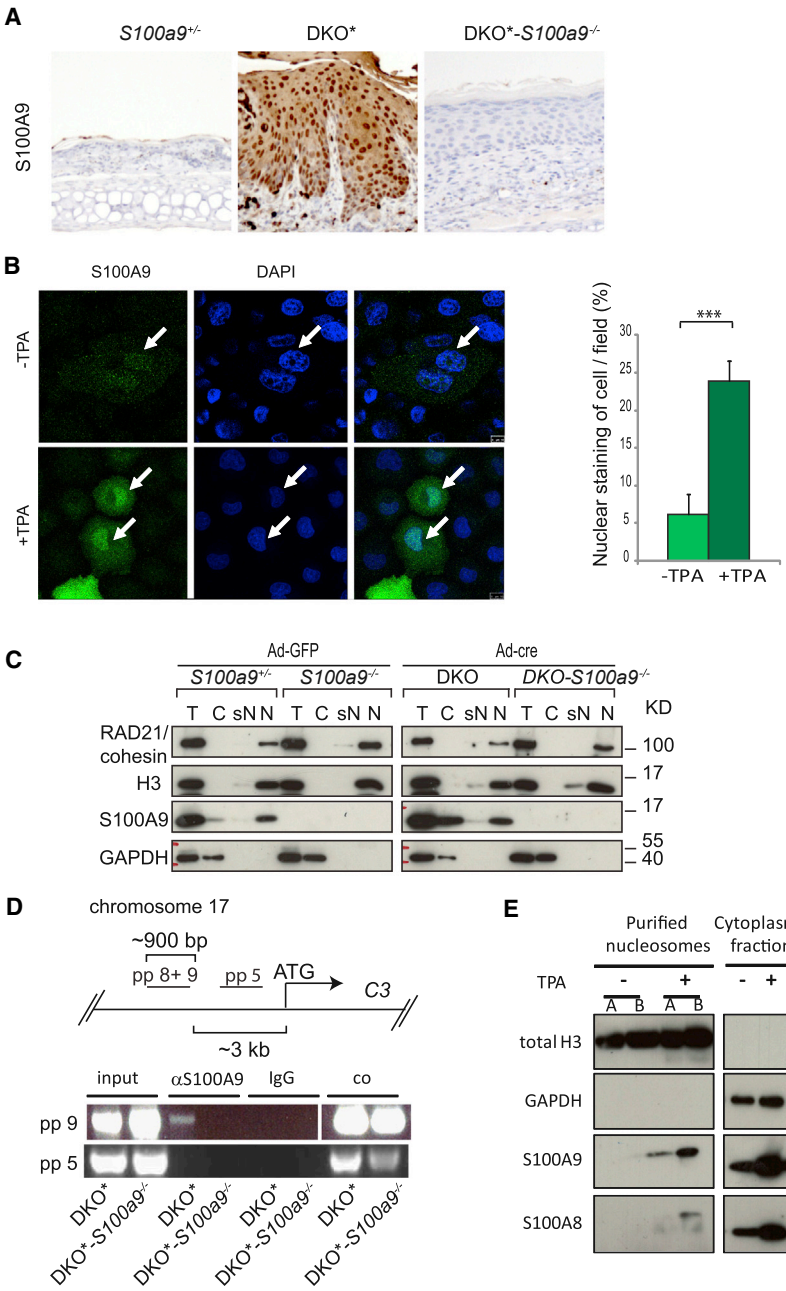

Figure 6. S100A9 as a Chromatin Component Modulating C3 Gene Expression

(A) IHC staining for S100A9 in ear samples of controls, DKO*, and DKO*-*S100a9*$^{-/-}$ mice (n = 10).

(B) Confocal analysis of IF staining for S100A9 in cultured human keratinocytes following TPA-stimulation for 3 hr (n = 3). Quantification of cells showing strong nuclear staining due to TPA treatment (12 randomly chosen fields and treatment) is shown. Error bars represent SD.

(C) Protein immunoblotting for RAD21/cohesin, Histone H3 (H3), S100A9, and GAPDH in cellular fractions of cultured mouse keratinocytes after Ad-cre deletion of *Jun* and *Junb* (DKO) and control cells (co); T, total cell extract; C, cytoplasmic fraction; sN, soluble nuclear fraction; N, chromatin enriched fraction (n = 4).

(D) Chromatin immunoprecipitation (ChIP) analysis for S100A9 on the C3 promoter region identified binding of S00A9 to an approximately 900 bp fragment upstream of the C3 translational start site (pp 9, primer pair 9; pp 5, primer pair 5; n = 4). Agarose gel electrophoresis pictures of the pp 9 amplicon showing a positive signal and pp 5 showing no binding of S100A9.

(E) Protein immunoblotting of Histone H3, GAPDH, S100A8, and S100A9 with nucleosome extracts from TPA stimulated primary mouse keratinocytes. As control, cytoplasmic fractions of the same cells were used; A, mono-nucleosome fraction; B, mono- and dinucleosome fraction (n = 6). See also Figure S6, Table S1, S2, and S4; Table S3.

Nuclear Function of S100A8-S100A9

Numerous reports describe the potential extracellular functions of S100A9/A8, although a nuclear function inferred from nuclear staining in different cell lines and psoriatic skin has not yet been reported (Barbe et al., 2008; Robinson and Hogg, 2000). IHC staining of highly inflamed mouse skin revealed strong nuclear localization of S100A9 in DKO* mice (Figure 6A). Moreover, confocal analysis of IF staining in human primary keratinocytes treated with TPA revealed a strong increase in nuclear compared to cytoplasmic S100A9 (Figure 6B). To further investigate the nuclear localization of S100A8-S100A9, we performed stepwise cellular fractionations. A strong increase in S100A9 in the nuclear fraction enriched for chromatin was seen in in vitro deleted DKO keratinocytes (Figure 6C). GAPDH was used as a marker for the cytoplasmic fraction and histone H3 and Rad21 as a marker for the chromatin fraction, showing a clean separation of the subcellular fractions (Figure 6C). These data suggest that S100A9 can be localized in the nucleus upon inflammatory stimuli.

To investigate whether the S100A9-dependent increase of C3 in DKO* epidermal samples, as well as in vitro-deleted DKO keratinocytes, was due to binding of S100A9 to DNA, we performed a chromatin immunoprecipitation (ChIP) for S100A9 by using in vitro-deleted DKO cells and DKO-*S100a9*$^{-/-}$ cells as controls (Figure 6D). Screening of a 5 kb upstream region, which was divided into approximately 500 bp fragments of the C3 promoter by ChIP analyses showed consistent binding of S100A9 to an approximately 900 bp fragment located 2,922 bp upstream of the ATG-start codon of the C3 gene (primer pairs 8 and 9 in Figure 6D; Figure S6A; Table S1). Neighboring regions did not show binding of S100A9 (primer pair 5, Figure 6D). Comparing the C3 promoter regions on human chromosome 19 and mouse chromosome 17 revealed a comparable composition. The approximately 900 bp fragment identified by ChIP for S100A9 is located almost the same distance to the C3 start site in human and mouse, approximately 2.8 kb and 2.6 kb, respectively.

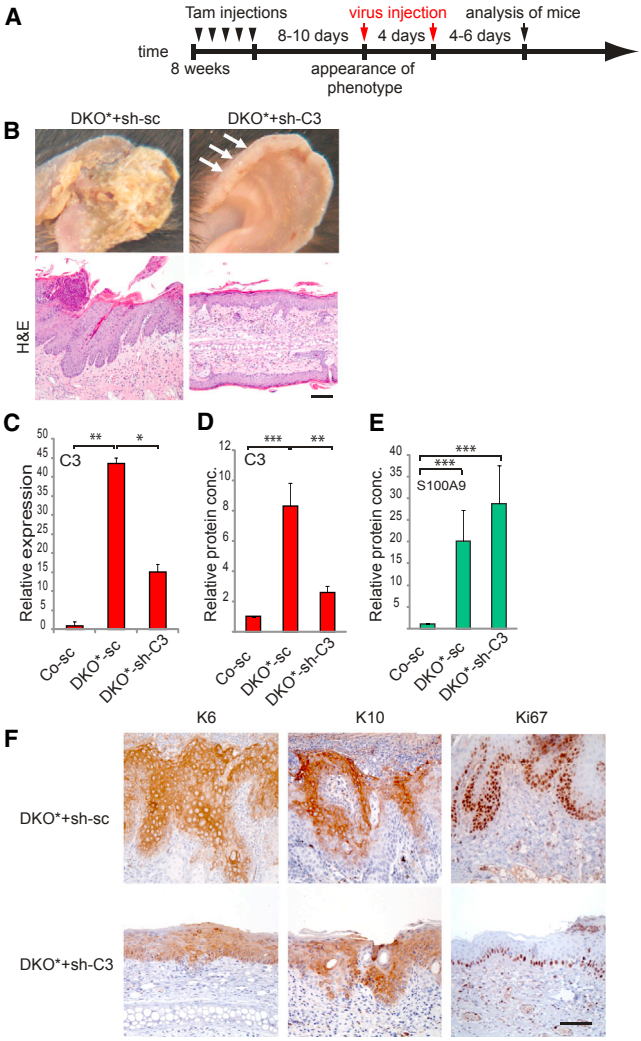

Figure 7. Downregulation of C3 Attenuates the Psoriasis-like Phenotype

(A) Experimental procedure blocking C3 with lentivirus-delivered shRNA against C3 and lentiviruses delivering GFP and scrambled RNAs as controls.

(B) Blocking C3 by intradermal injection of lentiviral shRNAs targeting C3 (sh-C3) into DKO* mice, displaying disease symptoms (n = 5), reduced the psoriasis-like phenotype compared to lentiviral scrambled RNA-injected (sh-sc) (n = 3) mice. H&E staining on ear sections of sh-sc and sh-C3 injected mice. Scale bar represents 50 μm.

(C and D) Analysis of C3 RNA and protein levels by RT-PCR and Selective Reaction Monitoring (SRM), respectively in extracts from total ear of scrambled- and shC3-injected mice. Error bars represent SD.

(E) A SRM MS analysis of S100A9 protein in scrambled- and shC3-injected mice.

(F) Analysis of the epidermal compartment in sh-sc and sh-C3 injected mice by IHC staining for keratin 6 (K6), keratin 10 (K10), and Ki67; scale bar represents 100 μm. See also Figure S7.

Furthermore, the 909 bp DNA fragment in the mouse C3 promoter region is highly similar to human (overall approximately 49.9% homology). It contains a sequence of a 153 bp subfragment, which shows an even higher homology (75%) between the human and mouse C3 promoter region (Figures S6A and S6B). Preliminary data from ChIP analyses on human keratinocytes also suggest binding of S100A9 to the human C3 promoter (data not shown).

To better define a putative function of S100A8-S100A9 in the nucleus, we performed immunoprecipitations (IPs) by using an antibody recognizing the heterodimer S100A8-S100A9 in mouse keratinocytes stimulated with TPA. The proteins obtained in the IP were analyzed by MS and the results were evaluated with IPA. This analysis identified a network of nuclear proteins including histones (Figure S6C; Table S2). We next isolated nucleosomes from cells treated with TPA to confirm binding of S100A8-S100A9 to histones. Mono- and dinucleosome fractions were analyzed by MS (Figure 6E; Figure S6C; Table S3). Importantly, S100A8-S100A9 was identified in the mono- and dinucleosome extracts by protein immunoblotting and by MS analyses (Figure S6C; Table S4). These results demonstrate a nuclear function of S100A9 possibly mediated by binding of S100A9 to histones and thereby regulating or influencing gene transcription.

Blocking C3 Is Therapeutically Beneficial

To investigate the potentially causal role of C3 in psoriasis, we subcutaneously injected lentivirus-delivered shRNAs targeting C3 8–10 days after initiating the disease, a time point at which the psoriasis-like phenotype is clearly visible (Figure 7A). To validate the efficacy of the lentiviral shRNA delivery in the mouse ear upon subcutaneous injections and to test for side effects, we also injected mice with lentiviruses expressing GFP or scrambled shRNA. A clear expression of GFP after lentiviral injection was seen both in controls and in DKO* mice (Figure S7A). No obvious side effects due to virus injections were observed (Figure S7B). Importantly, the psoriasis-like phenotype was virtually abolished, when C3 was knocked down in DKO* mice by injecting lentiviruses expressing shRNAs targeting C3 into the ear (Figure 7B). Only a slight thickening of the epidermis remained visible (Figure 7B), and C3 RNA and protein levels detected by SRM analysis were reduced in ears of lenti-shC3 injected mice compared to scramble controls (Figures 7C and 7D; data not shown). In contrast, CFB did not show a significant reduction in sh-C3 treated mice (Figure S7C). Protein levels of S100A8-S100A9 remained upregulated in sh-C3 treated DKO* mice (Figure 7E; Figure S7D), whereas RNA levels seemed to be reduced, although still increased in total ear of sh-C3 injected mice (Figure S7E). The observed decrease is likely due to reduced numbers of immune cells in these ears or reflects a feedback mechanism, which is inhibited by sh-C3 treatment. IHC analyses for keratin 6 and 10 as markers for stress response and epidermal differentiation showed reduced expression of K6 and a moderate improvement of K10 (Figure 7F). Ki67-positive cells in the basal epidermal layer of shC3-injected ears were reduced, but not completely normalized, reflecting the persisting epidermal thickening (Figure 7F). RNA expression of RANTES and CCL2, both C3 effectors, were strongly reduced in total ear of shC3-injected mice (Figures S7F and S7G). These data indicate that C3 plays a critical role in the psoriasis-like disease and that blocking C3 in psoriasis might be therapeutically beneficial.

DISCUSSION

Unbiased proteomic screening of the epidermal compartments from psoriatic patients and from genetic mouse models of

psoriasis have allowed us to identify a heretofore unappreciated functional link between S100A8-S100A9 and the alternative complement pathway C3-CFB. A remarkably similar protein expression pattern between diseased patient samples and epidermal mouse samples was observed, including a strong upregulation of S100A8-S100A9, IL-1β, and C3. Here we show that genetic deletion of S100A9 in the psoriasis-like mouse model reduced expression of complement factor C3 and its activation partner CFB, as well as IL-1β, thereby preventing the psoriasis-like disease. Moreover, a yet unknown chromatin association of S100A9 to the C3 promoter region was discovered in our study. Furthermore, blocking C3 in a mouse model attenuated the psoriasis-like phenotype.

Increased levels of S100A8-S100A9 in the psoriasis-like mouse model, as well as in keratinocytes, can be induced by epidermal deletion of *Junb* and *Jun* in vivo and in vitro. Loss of S100A8-S100A9 leads to prevention of the psoriasis-like symptoms, suggesting that this upregulation is a possible trigger for disease initiation. We propose that the changes in gene expression convert the keratinocytes into a ''primed'' state, being more sensitive to external stimuli, e.g., changes in skin microflora (Wolf et al., 2010; Wolf et al., 2011), facilitating the cellular increase of C3 in keratinocytes, and thereby activation of immune cells. Together C3 and CFB form the alternative complement pathway, which can be activated spontaneously by proteolysis, so called ''tick-over'' (Bexborn et al., 2008), or by bacterial surface antigens. Proteolytic activation of C3 occurs at low levels; if, however, C3 and CFB levels in keratinocytes are kept high due to upregulated S100A8-S100A9, tick-over events increase, leading to an imbalance in complement surveillance.

Both C3 and CFB belong to the complement network, which acts as an immune surveillance system able to discriminate healthy host tissue, cellular debris, and foreign pathogens. It has become apparent that any stimulus that affects the balance between complement activation and repression can cause inflammation and autoimmunity (Markiewski and Lambris, 2007). Keratinocytes are one of few cell types in the body that can produce S100A8-S100A9 and the complement factors C3 and CFB, making them potent activators of immune cells. Various insults like a barrier breakdown and bacterial invasion can lead to increased levels of these factors, signaling to the immune system that an immediate response is needed. Activated immune cells are effective producers of S100A8-S100A9 and C3, which in turn will amplify the signal dramatically and tissue levels of these factors can increase drastically. Several factors, including IL-17 produced by immune cells, will activate keratinocytes consequently leading to an autoamplification loop, which subsequently results in a chronic inflammatory state, as observed in diseases such as psoriasis.

The secretion of S100A8-S100A9 and C3 by keratinocytes and binding to their corresponding receptors, e.g., RAGE (damage associated molecular pattern molecules)-receptors or CD11b, on infiltrating immune cells stimulates these to produce additional inflammatory cytokines, like IL-17, MCP-1, and RANTES. We propose that induction of C3 by S100A8-S100A9 can lead to ''primed'' keratinocytes and subsequently to uncontrolled immune cell activation, angiogenesis, hyperproliferation of keratinocytes, and finally to the chronic inflammation that typifies psoriasis. Importantly, blocking C3 in the psoriasis-like mouse model diminished the psoriasis-like symptoms, implying that S100A8-S100A9 and C3 are not only serum markers for psoriasis severity, but likely serve as important amplifiers in psoriasis pathophysiology.

Until now S100A8-S100A9 proteins are mainly considered as chemoattractant proteins in mouse and antimicrobial in human. Our findings show that these proteins can be found in the chromatin enriched fraction in keratinocytes and can be implicated as modifiers of C3 transcription. It is not yet known how these proteins enter the nucleus, because no nuclear localization signal has been reported (Vogl et al., 2006). This is particularly interesting in the context of inflammatory stimuli, which induce besides a total increase of S100A9 a strong nuclear increase in primary keratinocytes. Our data indicate that the effect of S100A8-S100A9 on transcription is not achieved as a classical transcription factor, but rather through chromatin binding and remodeling. We show that S100A8-S100A9 proteins can interact in the nucleus with histones and nucleosomes, thereby possibly inducing epigenetic changes in gene expression. Future work will explore this activity of S100A8-S100A9 as well as whether these findings are applicable to other S100 proteins and other cell types, such as neutrophils.

Within the last decade, ''biological therapies'' have proven to be effective new treatments for inflammatory diseases. However, a concern about these treatments is the side effects of long-term chronic immune suppression, involving the potential to increase the risk of infection and cancer. Hence, development of effective drugs without these side effects that could be applied locally would be beneficial for psoriatic patients. As S100a9$^{-/-}$ mice are viable and show no skin phenotype, blocking S100A9 in psoriatic patients might be beneficial without impairing skin function. Interestingly, immunoglobulin-based drugs, which function as a sink for complement components, including C3 (Dalakas, 2004; Lutz et al., 2004), have emerged as effective long-term therapies in patients with autoimmune disease (Bayry et al., 2007). Case reports have shown that targeting C3 can also be beneficial for psoriatic patients (Gurmin et al., 2002). Moreover, a successful therapy for age-related macular degeneration (AMD) employed a C3 inhibitory peptide, which was locally injected into the retina (Ricklin and Lambris, 2008). This C3 inhibitory peptide is unfortunately not active in rodents (Ricklin and Lambris, 2008) and hence cannot be evaluated in mouse models. Blocking the C3 receptor CD11b has also been shown to reduce inflammation in a T cell-dependent inflammation mouse model, supporting the notion that blocking C3 could be beneficial for psoriatic patients (Leon et al., 2006). The fact that C3 and CFB have an extracellular function and are activated locally makes them attractive targets. The activation of the complement system, being a potent activator of the blood coagulation or fibrinolysis regulatory cascade, might also explain the local and precise borders of the inflammatory plaques, seen in psoriasis. In conclusion, inhibitory strategies for S100A8-S100A9 and/or C3 have exciting potential to become effective new therapeutics for psoriasis.

EXPERIMENTAL PROCEDURES

Mouse Strains and Treatment

Mice carrying *Junb* and *Jun* alleles flanked by loxP sites and the K5-CreER^{T} allele were used in this study (Zenz et al., 2005). The *S100a9*$^{-/-}$ mouse strain

was obtained from Nancy Hogg (Hobbs et al., 2003). Eight-week-old mice were treated with Tamoxifen (1 mg/day) for 5 consecutive days by intraperitoneal injections with 1 mg tamoxifen (Sigma) to induce the deletion of the two genes in the epidermis (these mice are referred to as DKO*). All mice were on a mixed genetic background originally derived from F1 (129/BL/6) intercrosses for an extensive period of time (over 6 years) with a very robust and stable phenotype; only littermate controls were used. Controls (*Junb*$^{f/f}$; *Jun*$^{f/f}$; *S100a9*$^{+/-}$), *S100a9*$^{-/-}$ (*Junb*$^{f/f}$; *Jun*$^{f/f}$; *S100a9*$^{-/-}$), DKO* (JunB$^{\Delta ep/\Delta ep}$; *Jun*$^{\Delta ep/\Delta ep}$; *S100a9*$^{+/+}$ or *Junb*$^{\Delta ep/\Delta ep}$; *Jun*$^{\Delta ep/\Delta ep}$; *S100a9*$^{+/-}$) and DKO*-*S100a9*$^{-/-}$ (*Junb*$^{\Delta ep/\Delta ep}$; *Jun*$^{\Delta ep/\Delta ep}$; *S100a9*$^{-/-}$). All mouse experiments were performed in accordance with local and institutional regulations and licenses.

Statistical Analysis

Data are shown as mean + SD and were analyzed with a two-sided, unpaired Student's t test. Differences were considered statistically significant when p* < 0.05 and the asterisk indicate *p < 0.05; **p < 0.005; ***p < 0.0005.

Imiquimod Treatment

Nine- to 11-week-old *S100a9*$^{-/-}$ mice and control siblings received a daily topical dose of 50 mg of commercially available Imiquimod cream (5%; Aldara; 3M Pharmaceuticals) on the shaved back. Control mice were treated similarly with a control vehicle cream. Mice were treated for 6 consecutive days. Samples were taken 1 day after the last treatment.

Patient Samples

Nonlesional and lesional samples were biopsied only after informed consent to the patients and following the approval by the Ethics Committee of the Hospital La Princesa, Madrid, Spain.

Immunohistochemistry and Immunofluorescence

At day 23 of the study, mice were sacrificed and their ears were collected and cut in half. One half of each ear was processed for paraffin sections, the other half was embedded in optimal cutting temperature (OCT) compound (Sakkura Finetek, Torrance, CA), snap-frozen in liquid nitrogen, and 4 μm cryostat sections were cut. Immunohistological analyses were performed as described previously by using the following antibodies: CD4 and CD8 (BD Biosciences), Alexa488- or Alexa594-coupled secondary antibodies (Invitrogen). Hoechst 33342 (Invitrogen) was used for nuclear stains. For paraffin embedding, tissues were fixed in 3.7% paraformaldehyde (PFA) in PBS (pH 7.2) at 4°C overnight. Before standard dehydration and paraffin infiltration, the tissue was washed in PBS. Three micrometer sections of formalin-fixed samples were processed for hematoxylin and eosin stains (H&E) according to standard procedures. Immunohistochemistry (IHC) with antibodies against anti-mouse keratin 6 and keratin 10 (all from Covance Research Products), S100A8 and S100A9 (both Santa Cruz), Ki67 (Novocastra), and F4-80 (Santa Cruz) was performed as previously described. Staining for myeloid peroxidase (MPO) was performed as described in Zenz et al. (2005).

The IHC stainings on human paraffin sections were done using anti-human S100A8-S100A9 (calprotectin, Clone MAC 387, DAKO) and anti-human C3 (F-0201, DAKO) and CD45 (2B11+PD7/26, DAKO) according to the manufacturer's protocol.

The following methods are described in detail in Supplemental Information. Skin samples were isolated and epidermis was separated from dermis and analyzed by iTRAQ and for mRNA (quantitative PCR with reverse transcription) and protein determination (immunoblotting). Immunocytochemistry was performed on paraformaldehyde fixed paraffin embedded skin sections. Primary mouse keratinocytes were isolated and cultured. ELISAs were performed according to the manufacturer's protocols. Cell fractionation and ChIP procedures and adoptive bone marrow transfer are described in the Supplemental Information.

Proteomic Analysis of Nucleosome Extracts

Proteins in nucleosome extracts were digested with a modified FASP protocol. Peptides were separated by online nano-LC and analyzed by electrospray MS/MS with a LTQ Orbitrap Velos mass spectrometer (Thermo Scientific). Raw files were searched against UniProtKB/Swiss-Prot mouse database (release date: January, 2013 50517 entries) with MASCOT2 as a search engine through the Proteome Discoverer (Thermo Scientific) software. Peptides and were filtered at 1% FDR with a concatenated database. A more detailed description of methodology is provided in the Supplemental Information.

SUPPLEMENTAL INFORMATION

Supplemental Information includes seven figures, four tables, Supplemental Experimental Procedures and can be found with this article online at http://dx.doi.org/10.1016/j.immuni.2013.11.011.

ACKNOWLEDGMENTS

We are very grateful to Peter Angel, Doug Hanahan, Mirna Pérez-Moreno, Mercedes Rincon, Ethan Shevach, Maria Sibilia, Erwin Tschachler, Ronald Wolf, and members of the Wagner laboratory for discussions and critically reading the manuscript. We thank Thomas Jenuwein for advice and critical discussions regarding the role of S100 proteins in the nucleus. We would also like to thank Maria Helena Idarraga-Amado and Maria Martin for excellent technical support and Diego Megías from the CNIO Confocal Microscopy unit and the CNIO Proteomics unit for outstanding technical assistance. We are grateful to Esteban Daudén for providing psoriasis tissue samples. The project was initiated at the IMP, which is funded by Boehringer Ingelheim, and was supported by an Austrian Science Foundation grant NFN S94-SP11. E.F.W. is funded by the Banco Bilbao Vizcaya Argentaria (BBVA) Foundation and a European Research Council Advanced Grant (ERC FCK/2008/37).

Received: February 17, 2013
Accepted: October 21, 2013
Published: December 12, 2013

REFERENCES

Abtin, A., Eckhart, L., Gläser, R., Gmeiner, R., Mildner, M., and Tschachler, E. (2010). The antimicrobial heterodimer S100A8/S100A9 (calprotectin) is upregulated by bacterial flagellin in human epidermal keratinocytes. J. Invest. Dermatol. *130*, 2423–2430.

Acevedo, F., and Hammar, H. (1989). Complement C3 proteins in psoriasis. Br. J. Dermatol. *121*, 329–335.

Arwert, E.N., Hoste, E., and Watt, F.M. (2012). Epithelial stem cells, wound healing and cancer. Nat. Rev. Cancer *12*, 170–180.

Baker, J.R., Jeffery, R., May, R.D., Mathies, M., Spencer-Dene, B., Poulsom, R., and Hogg, N. (2011). Distinct roles for S100a8 in early embryo development and in the maternal deciduum. Dev. Dyn. *240*, 2194–2203.

Barbe, L., Lundberg, E., Oksvold, P., Stenius, A., Lewin, E., Björling, E., Asplund, A., Pontén, F., Brismar, H., Uhlén, M., and Andersson-Svahn, H. (2008). Toward a confocal subcellular atlas of the human proteome. Mol. Cell. Proteomics *7*, 499–508.

Basset-Séguin, N., Porneuf, M., Dereure, O., Mils, V., Tesnières, A., Yancey, K.B., and Guilhou, J.J. (1993). C3d,g deposits in inflammatory skin diseases: use of psoriatic skin as a model of cutaneous inflammation. J. Invest. Dermatol. *101*, 827–831.

Bayry, J., Lacroix-Desmazes, S., Kazatchkine, M.D., and Kaveri, S.V. (2007). Monoclonal antibody and intravenous immunoglobulin therapy for rheumatic diseases: rationale and mechanisms of action. Nat. Clin. Pract. Rheumatol. *3*, 262–272.

Bexborn, F., Andersson, P.O., Chen, H., Nilsson, B., and Ekdahl, K.N. (2008). The tick-over theory revisited: formation and regulation of the soluble alternative complement C3 convertase (C3(H2O)Bb). Mol. Immunol. *45*, 2370–2379.

Dalakas, M.C. (2004). Intravenous immunoglobulin in autoimmune neuromuscular diseases. JAMA *291*, 2367–2375.

Di Meglio, P., Perera, G.K., and Nestle, F.O. (2011). The multitasking organ: recent insights into skin immune function. Immunity *35*, 857–869.

Gebhardt, C., Németh, J., Angel, P., and Hess, J. (2006). S100A8 and S100A9 in inflammation and cancer. Biochem. Pharmacol. *72*, 1622–1631.

Gebhardt, C., Riehl, A., Durchdewald, M., Németh, J., Fürstenberger, G., Müller-Decker, K., Enk, A., Arnold, B., Bierhaus, A., Nawroth, P.P., et al. (2008). RAGE signaling sustains inflammation and promotes tumor development. J. Exp. Med. *205*, 275–285.

Grivennikov, S.I., Greten, F.R., and Karin, M. (2010). Immunity, inflammation, and cancer. Cell *140*, 883–899.

Guinea-Viniegra, J., Zenz, R., Scheuch, H., Hnisz, D., Holcmann, M., Bakiri, L., Schonthaler, H.B., Sibilia, M., and Wagner, E.F. (2009). TNFalpha shedding and epidermal inflammation are controlled by Jun proteins. Genes Dev. *23*, 2663–2674.

Gurmin, V., Mediwake, R., Fernando, M., Whittaker, S., Rustin, M.H., and Beynon, H.L. (2002). Psoriasis: response to high-dose intravenous immunoglobulin in three patients. Br. J. Dermatol. *147*, 554–557.

Guttman-Yassky, E., Lowes, M.A., Fuentes-Duculan, J., Zaba, L.C., Cardinale, I., Nograles, K.E., Khatcherian, A., Novitskaya, I., Carucci, J.A., Bergman, R., and Krueger, J.G. (2008). Low expression of the IL-23/Th17 pathway in atopic dermatitis compared to psoriasis. J. Immunol. *181*, 7420–7427.

Hobbs, J.A., May, R., Tanousis, K., McNeill, E., Mathies, M., Gebhardt, C., Henderson, R., Robinson, M.J., and Hogg, N. (2003). Myeloid cell function in MRP-14 (S100A9) null mice. Mol. Cell. Biol. *23*, 2564–2576.

Javkhlan, P., Hiroshima, Y., Azlina, A., Hasegawa, T., Yao, C., Akamatsu, T., Kido, J., Nagata, T., and Hosoi, K. (2011). Lipopolysaccharide-mediated induction of calprotectin in the submandibular and parotid glands of mice. Inflammation *34*, 668–680.

Johansen, C., Kragballe, K., Rasmussen, M., Dam, T.N., and Iversen, L. (2004). Activator protein 1 DNA binding activity is decreased in lesional psoriatic skin compared with nonlesional psoriatic skin. Br. J. Dermatol. *151*, 600–607.

Kerkhoff, C., Voss, A., Scholzen, T.E., Averill, M.M., Zänker, K.S., and Bornfeldt, K.E. (2012). Novel insights into the role of S100A8/A9 in skin biology. Exp. Dermatol. *21*, 822–826.

Leon, F., Contractor, N., Fuss, I., Marth, T., Lahey, E., Iwaki, S., la Sala, A., Hoffmann, V., Strober, W., and Kelsall, B.L. (2006). Antibodies to complement receptor 3 treat established inflammation in murine models of colitis and a novel model of psoriasiform dermatitis. J. Immunol. *177*, 6974–6982.

Leukert, N., Vogl, T., Strupat, K., Reichelt, R., Sorg, C., and Roth, J. (2006). Calcium-dependent tetramer formation of S100A8 and S100A9 is essential for biological activity. J. Mol. Biol. *359*, 961–972.

Lowes, M.A., Bowcock, A.M., and Krueger, J.G. (2007). Pathogenesis and therapy of psoriasis. Nature *445*, 866–873.

Lutz, H.U., Stammler, P., Bianchi, V., Trüeb, R.M., Hunziker, T., Burger, R., Jelezarova, E., and Späth, P.J. (2004). Intravenously applied IgG stimulates complement attenuation in a complement-dependent autoimmune disease at the amplifying C3 convertase level. Blood *103*, 465–472.

Manitz, M.P., Horst, B., Seeliger, S., Strey, A., Skryabin, B.V., Gunzer, M., Frings, W., Schönlau, F., Roth, J., Sorg, C., and Nacken, W. (2003). Loss of S100A9 (MRP14) results in reduced interleukin-8-induced CD11b surface expression, a polarized microfilament system, and diminished responsiveness to chemoattractants in vitro. Mol. Cell. Biol. *23*, 1034–1043.

Markiewski, M.M., and Lambris, J.D. (2007). The role of complement in inflammatory diseases from behind the scenes into the spotlight. Am. J. Pathol. *171*, 715–727.

Monsinjon, T., Gasque, P., Chan, P., Ischenko, A., Brady, J.J., and Fontaine, M.C. (2003). Regulation by complement C3a and C5a anaphylatoxins of cytokine production in human umbilical vein endothelial cells. FASEB J. *17*, 1003–1014.

Nacken, W., Roth, J., Sorg, C., and Kerkhoff, C. (2003). S100A9/S100A8: Myeloid representatives of the S100 protein family as prominent players in innate immunity. Microsc. Res. Tech. *60*, 569–580.

Nakatsuji, T., and Gallo, R.L. (2011). Antimicrobial Peptides: Old Molecules with New Ideas. J. Invest. Dermatol. *132*, 887–895.

Németh, J., Stein, I., Haag, D., Riehl, A., Longerich, T., Horwitz, E., Breuhahn, K., Gebhardt, C., Schirmacher, P., Hahn, M., et al. (2009). S100A8 and S100A9 are novel nuclear factor kappa B target genes during malignant progression of murine and human liver carcinogenesis. Hepatology *50*, 1251–1262.

Nestle, F.O., Kaplan, D.H., and Barker, J. (2009). Psoriasis. N. Engl. J. Med. *361*, 496–509.

Palamara, F., Meindl, S., Holcmann, M., Lührs, P., Stingl, G., and Sibilia, M. (2004). Identification and characterization of pDC-like cells in normal mouse skin and melanomas treated with imiquimod. J. Immunol. *173*, 3051–3061.

Ricklin, D., and Lambris, J.D. (2008). Compstatin: a complement inhibitor on its way to clinical application. Adv. Exp. Med. Biol. *632*, 273–292.

Robinson, M.J., and Hogg, N. (2000). A comparison of human S100A12 with MRP-14 (S100A9). Biochem. Biophys. Res. Commun. *275*, 865–870.

Schonthaler, H.B., Huggenberger, R., Wculek, S.K., Detmar, M., and Wagner, E.F. (2009). Systemic anti-VEGF treatment strongly reduces skin inflammation in a mouse model of psoriasis. Proc. Natl. Acad. Sci. USA *106*, 21264–21269.

Suzuki, H., Wang, B., Shivji, G.M., Toto, P., Amerio, P., Tomai, M.A., Miller, R.L., and Sauder, D.N. (2000). Imiquimod, a topical immune response modifier, induces migration of Langerhans cells. J. Invest. Dermatol. *114*, 135–141.

Swamy, M., Jamora, C., Havran, W., and Hayday, A. (2010). Epithelial decision makers: in search of the 'epimmunome'. Nat. Immunol. *11*, 656–665.

Tohyama, M., Hanakawa, Y., Shirakata, Y., Dai, X., Yang, L., Hirakawa, S., Tokumaru, S., Okazaki, H., Sayama, K., and Hashimoto, K. (2009). IL-17 and IL-22 mediate IL-20 subfamily cytokine production in cultured keratinocytes via increased IL-22 receptor expression. Eur. J. Immunol. *39*, 2779–2788.

van der Fits, L., Mourits, S., Voerman, J.S., Kant, M., Boon, L., Laman, J.D., Cornelissen, F., Mus, A.M., Florencia, E., Prens, E.P., and Lubberts, E. (2009). Imiquimod-induced psoriasis-like skin inflammation in mice is mediated via the IL-23/IL-17 axis. J. Immunol. *182*, 5836–5845.

van Lent, P.L., Hofkens, W., Blom, A.B., Grevers, L., Sloetjes, A., Takahashi, N., van Tits, L.J., Vogl, T., Roth, J., de Winther, M.P., and van den Berg, W.B. (2009). Scavenger receptor class A type I/II determines matrix metalloproteinase-mediated cartilage destruction and chondrocyte death in antigen-induced arthritis. Arthritis Rheum. *60*, 2954–2965.

Venkatesha, R.T., Berla Thangam, E., Zaidi, A.K., and Ali, H. (2005). Distinct regulation of C3a-induced MCP-1/CCL2 and RANTES/CCL5 production in human mast cells by extracellular signal regulated kinase and PI3 kinase. Mol. Immunol. *42*, 581–587.

Vogl, T., Leukert, N., Barczyk, K., Strupat, K., and Roth, J. (2006). Biophysical characterization of S100A8 and S100A9 in the absence and presence of bivalent cations. Biochim. Biophys. Acta *1763*, 1298–1306.

Wagner, E.F., Schonthaler, H.B., Guinea-Viniegra, J., and Tschachler, E. (2010). Psoriasis: what we have learned from mouse models. Nat Rev Rheumatol *6*, 704–714.

Wolf, R., Mascia, F., Dharamsi, A., Howard, O.M., Cataisson, C., Bliskovski, V., Winston, J., Feigenbaum, L., Lichti, U., Ruzicka, T., et al. (2010). Gene from a psoriasis susceptibility locus primes the skin for inflammation. Sci. Transl. Med. *2*, 61ra90.

Wolf, R., Ruzicka, T., and Yuspa, S.H. (2011). Novel S100A7 (psoriasin)/S100A15 (koebnerisin) subfamily: highly homologous but distinct in regulation and function. Amino Acids *41*, 789–796.

Wyatt, R.J., Wang, C., Hudson, E.C., Jones, R.M., Noah, P.W., and Rosenberg, E.W. (1989). Complement phenotypes in patients with psoriasis. Hum. Hered. *39*, 327–332.

Zenz, R., Eferl, R., Kenner, L., Florin, L., Hummerich, L., Mehic, D., Scheuch, H., Angel, P., Tschachler, E., and Wagner, E.F. (2005). Psoriasis-like skin disease and arthritis caused by inducible epidermal deletion of Jun proteins. Nature *437*, 369–375.

Zenz, R., Eferl, R., Scheinecker, C., Redlich, K., Smolen, J., Schonthaler, H.B., Kenner, L., Tschachler, E., and Wagner, E.F. (2008). Activator protein 1 (Fos/Jun) functions in inflammatory bone and skin disease. Arthritis Res. Ther. *10*, 201.